

NUMERICAL SIMULATION OF DUPLEX STEEL MULTIPASS WELDING

Analyses based on FEM calculations have significantly changed the possibilities of determining welding strains and stresses at early stages of product design and welding technology development. Such an approach to design enables obtaining significant savings in production preparation and post-weld deformation corrections and is also important for utility properties of welded joints obtained. As a result, it is possible to make changes to a simulated process before introducing them into real production as well as to test various variants of a given solution. Numerical simulations require the combination of problems of thermal, mechanical and metallurgical analysis. The study presented involved the SYSWELD software-based analysis of GMA welded multipass butt joints made of duplex steel sheets. The analysis of the distribution of stresses and displacements were carried out for typical welding procedure as during real welding tests.

Keywords: FEM, SYSWELD, welding strains, welding stresses, GMA, duplex steel

1. Introduction

The numerical simulation of welding processes is one of the more complicated issues in analyses carried out using the Finite Element Method. It is because of a big number of factors taking into consideration. A welding process thermal cycle directly affects the thermal and mechanical behaviour of a structure during the process. High process temperature and subsequent cooling of elements being welded generate undesirable strains and stresses in the structure being made. For this reason, it is necessary to possess extensive knowledge related to the behaviour of materials subjected to welding thermal cycles. Obtaining such data requires not only vast knowledge but also access to a wide range of laboratory examination focused on the mechanical and thermo-metallurgical properties of the materials used. Also knowledge concerning the welding process itself and the proper selection of boundary conditions poses a significant challenge for engineers wishing to apply this area of knowledge in their practical studies [1,2]. However, even vast theoretical knowledge, often supported by extensive laboratory tests, is not sufficient for obtaining high accuracy of numerical analysis results using accidental tools. Software is of vital importance here.

A short product life cycle between subsequent changes of models or solutions makes classical prototyping unprofitable and often unfeasible due to time restrictions and the quickly increasing complexity of products manufactured today [1,3-5]. More than a decade ago 3D engineering software opened engineering personnel to new possibilities. Equally beneficial was the market introduction of advanced calculation packages based on the Finite Element method and creating the “new quality” in designing countless versions of details aimed to

obtain the maximum quality, durability and specific utility features. Additional specialization of such packages makes their use significantly more flexible and complete within the industries for which they have been intended. Ready-made solutions provided to engineers working on new products offer quick and unambiguous answers to questions posed not only by engineers but also by economists actively participating in designing equipment and machinery elements [1,6,10].

The research conducted involved the use of the SYSWELD software package developed by the ESI Group. This software enables FEM-based simulations including welding and heat treatment issues. SYSWELD covers all the problems related to non-linear analyses, i.e. non-linear heat conduction in every space, non-linear geometry of great strains, isotropic and kinematic metal hardening or phase transformations. Combining the influence of such a great number of phenomena taking place during a welding process makes it possible to obtain the mentioned high compatibility of simulation results with the actual behaviour of an element or structure. SYSWELD enables the simulation of welding processes within a very wide range, i.e. both with and without filler metals, for heat sources having (friction welding, spot welding) and not having (electric arc, laser beam, electron beam) physical contact with the element being welded. The range of simulating heat treatment is equally wide and includes, among others, tempering, (laser, induction, electron beam, plasma, friction) hardening, carbonizing and nitriding. Computational process input data are the following:

- method used in a welding process,
- welding process linear energy/welding process parameters,
- geometry of an element/structure being welded (import

* UNIVERSITY OF TECHNOLOGY AND LIFE SCIENCE, MATERIAL ENGINEERING UNIT, MECHANICAL ENGINEERING DEPARTMENT, IN BYDGOSZCZ, 7 PROF. S. KALISKIEGO STR., 85-796 BYDGOSZCZ, POLAND

** SILESIAN UNIVERSITY OF TECHNOLOGY, DEPARTMENT OF WELDING, FACULTY OF MECHANICAL ENGINEERING, 18AKONARSKIEGO STR., 44-100GLIWICE, POLAND

Corresponding author: tgietka@utp.edu.pl

from popular CAD systems in Pro/E, CATIA, UG, I-DEAS, Patran, Ansys, IGES, STL, STEP formats etc.),

- material,
- preheating temperature,
- number of runs/joints and their location and sequence,
- manner of stiffening/fixing a structure to be welded,
- post-weld heat treatment parameters, if any, etc.

Equally important are results obtained by means of simulation, such as:

- temperature field and gradients,
- contents of phases in the individual areas of a joint,
- strains,
- internal stresses,
- displacements,
- hardness [1,10].

2. Problem description

During a welding process, the heat source supplies a specific amount of energy to the material being welded. As a result, the material undergoes partial expansion, yet this movement is partly limited by elements being welded, by the base on which these elements are rested and by the fixtures of a welding stand. Consequently, thermal stresses are generated in the welding area. While temperature increases, a plasticized material undergoes plastic deformation, which after cooling of a joint generates stresses and strains of elements welded.

Stresses generated in a welded joint depend, among others, on the manner in which a structure is stiffened during a welding process. A high structure stiffening degree generates slight strains at the cost of the high level of stresses and, vice versa, a low structure stiffening degree causes a significant decrease in these stresses resulting in a significant increase in welding strains. This entails the necessity of developing a technology for the optimum fixing of elements to be welded, i.e. reducing the level of post-weld stresses while at the same time maintaining a low level of strains. Otherwise, it may become necessary to use another procedure in a production process, i.e. straightening, which however, can be costly and sometimes even unfeasible. The problem of modelling welding processes using FEM is complex. The determination of the level of welding stresses, strains and temperature field distribution is highly complicated due to the complex character of dependences between temperature, shrinkage, thermal expansion and variable material properties in time and space. In order to simplify the analysis, thermal and mechanical states are often analysed separately. This approach is dictated by an adopted principle, according to which changes in the mechanical state (stresses and strains) do not change process temperature, whereas a change in temperature is clearly reflected in the changing distribution of strains and stresses. For this reason, the first analysis of a welding process in such a case is concerned with the distribution of temperature fields during a welding process. The results are then used to determine the changes in the distribution of stresses and strains. Such a type of analysis

is based on an assumption that heat generated during plastic deformation is significantly lower than heat supplied by an electric arc. That is why it is possible to carry out thermal and mechanical analysis as two separate analyses one after the other [1-5].

Another crucial issue in numerical analysis is the manner of describing how heat is supplied to a welded joint. Reference publications related to the numerical modelling of welding processes contain, among others, the 2D-Gaussian surface heat source model (2D Gauss), the double-ellipsoidal heat source model (so-called Goldak's model) or the 3D-Gaussian conical heat source model. Each of these sources has its own application in modelling a specific welding process or heat treatment. A Surface heat source can be successfully used in modelling heat treatment processes, gas welding processes or MMA welding processes. The Goldak's model proves useful in situations where a process is carried out using "melt-in welding" and the possibilities of changing the shape of a model enable its adjustment to a specific welding method. In turn, the conical model successfully represents welding methods characterized by high energy and deep penetration. An example of these applications can be laser or electron beam welding using "key-hole welding" [1,7-9].

3. Real welding tests

As a filler material during experiments of X2CrNiMoN22-5-3 steel plates multipass welding, flux cored wire AVESTA FCW 2205 with diameter 1,2 mm was used. Test specimens were prepared according to PN EN 15614-1 standard requirements. Groove preparation method and welding sequence scheme are shown at Fig. 1.

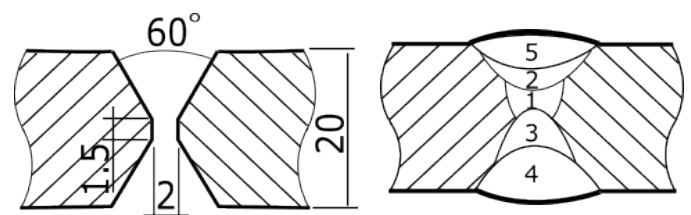


Fig. 1. Groove preparation and welding sequence scheme

In parallel with numerical analyses, from welded joints were cut two specimens for real mechanical properties tests according to PN-EN ISO 4136: 2013-05 standard. Results of tensile strength tests with maximal forces and place of break were shown at Table 3.

Microstructure of real welded joints in base material, HAZ and weld areas was shown at Figure 2. There is a visible difference between the morphology of ferrite and austenite precipitations in different areas of the welded joints. Significant difference is also phase contribution on these areas. Of course it depends on many conditions as: welding method, welding position and parameters [11,12]. Ferrite- δ content measured on Feritscope FMP30 at face and root of welded joint according to PN- EN ISO 17655 standards was shown at Table 4.

TABLE 1

Chemical composition, thermal and mechanical properties of X2CrNiMoN22-5-3 steel

Designation according to 10027-1: X2CrNiMoN22-5-3 according to 10027-2: 1.4462	C % max	Si %	Mn %	P %max	S %max	N %	Cr %	Mo %	Ni %
	0.030	≤1.00	≤2.00	0.035	0.015	0.10 ÷ 0.22	21.0 ÷ 23.0	2.50 ÷ 3.50	4.50 ÷ 6.50
Density, kg/dm ³	Elasticity coefficient, GPa				Average thermal expansion coefficient, 10 ⁻⁶ · K ⁻¹				
	7.80	20°C 200	100°C 194	200°C 186	300°C 180	100°C 13.0	200°C 13.5	300°C 14.0	
Thermal conductivity at 20°C W/m · K	Unit thermal capacity at 20°C J/kg · K			Electrical resistivity at 20°C Ω · mm ² /m		Magnetisability			
15	500			0.8		YES			

TABLE 2

Welding parameters of X2CrNiMoN22-5-3 steel 20 mm thickness butt weld joint multipasswelding, Fig. 1

Bead number:	1	2	3	4	5
Interpass temp., °C	110	50	140	130	-
Arc voltage, V	28.7	29.3	34.0	28.3	28.3
Welding current, A	216	213	265	203	202
Weld length, mm	400	400	400	400	400
Welding time, s	104	88	112	135	110
Wire feed speed, m/min	10.0	10.7	16.9	9.0	9.0
Heat input, J/mm	1614	1386	2523	1940	1574

REMARKS: Welded plates were joined before welding with two tack welds at the beginning and the end of the weld path. During welding and after there is no additional clamping equipment

TABLE 3

Results of static tensile strength tests for transverse stretch test of welded joints specimens

No.	Identification of sample	Type of sample acc. PN-EN ISO 4136	Dimensions		So mm ²	Fm kN	Rm MPa	Place of brake
			ao mm	bo mm				
1	PA20_(1)	Fig. 1	20.71	29.51	661.15	485.0	793.58	BASE MATERIAL
2	PA20_(2)		20.60	29.39	605.43	480.0	792,82	BASE MATERIAL

TABLE 4

Volumetric amount of ferrite delta measured on face and root of welded joint

No.	Identification of sample	Side of test	Ferrite-δ content, % vol.				
			BASE MATERIAL	HAZ	WELD	HAZ	BASE MATERIAL
1	PA20_(1)	from face side	35	32	34	32	36
			36	31	35	32	35
			36	31	34	31	36
2	PA20_(2)	from root side	35	34	36	33	35
			36	34	36	34	35
			35	33	36	33	35

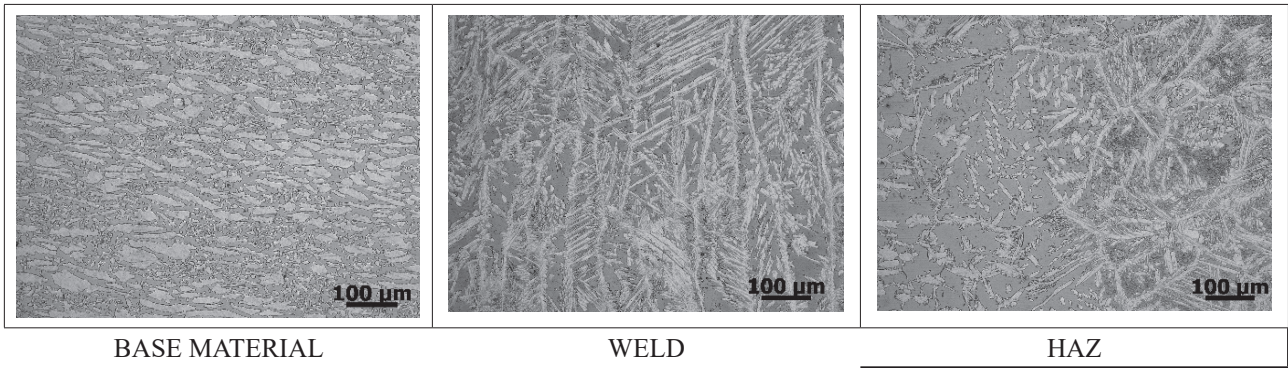


Fig. 2 Microstructure of X2CrNiMoN22-5-3 steel multipass butt weld joint t: a) base material, b) weld, c) heat affected zone

4. Numerical simulations results

For numerical welding simulation a discrete model was prepared. Dimensions of simulated weld joint were in accordance with PN EN 15614-1 standards. Mesh of finite elements contains 64648 3D solid type elements and 50704 nodes, Fig. 3. To increase precision of the calculation, mesh was refined in the area of welded joint and HAZ. As a heat source model, Goldak’s double ellipsoid heat source model was used. This heat source model was calibrated using „Heat Input Fitting” module in SYSWELD to obtain the results similar to the real welding tests, Fig. 4.

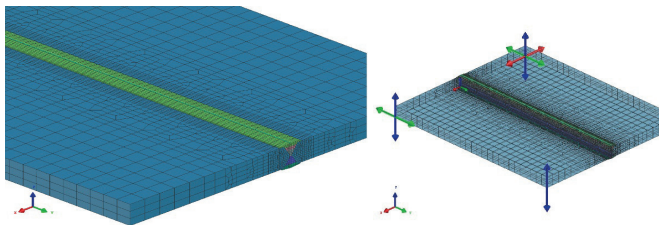


Fig. 3. Three-dimensional, numerical butt weld joint model and clamping conditions used during welding

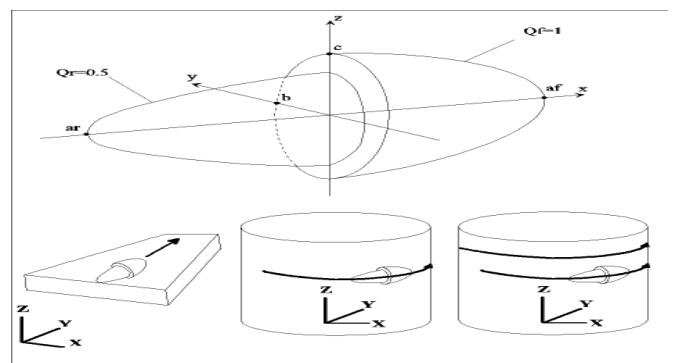


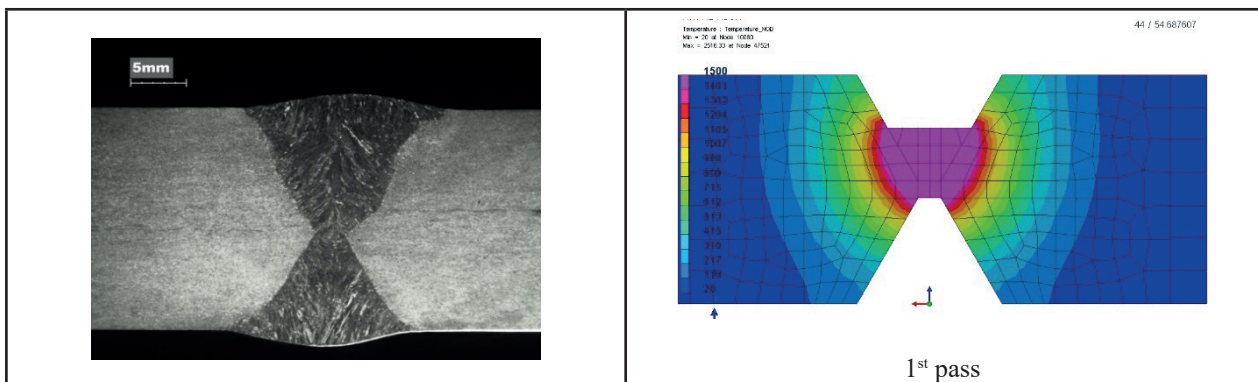
Fig. 4. Double ellipsoid heat source model

Goldak’s heat source model is built from two ellipsoids described with equations:

$$Q(x, y, z) = Q_f \exp\left(-\left(\frac{x^2}{a_f^2} + \frac{y^2}{b^2} + \frac{z^2}{c^2}\right)\right) \quad \text{front part of model}$$

$$Q(x, y, z) = Q_r \exp\left(-\left(\frac{x^2}{a_r^2} + \frac{y^2}{b^2} + \frac{z^2}{c^2}\right)\right) \quad \text{rear part of model}$$

where: Q_f and Q_r are the maximal power density for front and rear part of the model respectively, a_f , a_r , b and c are parameters responsible on heat source geometry changes and fitting the shape of heat source model to the results of real welding tests, Fig. 4 [10].



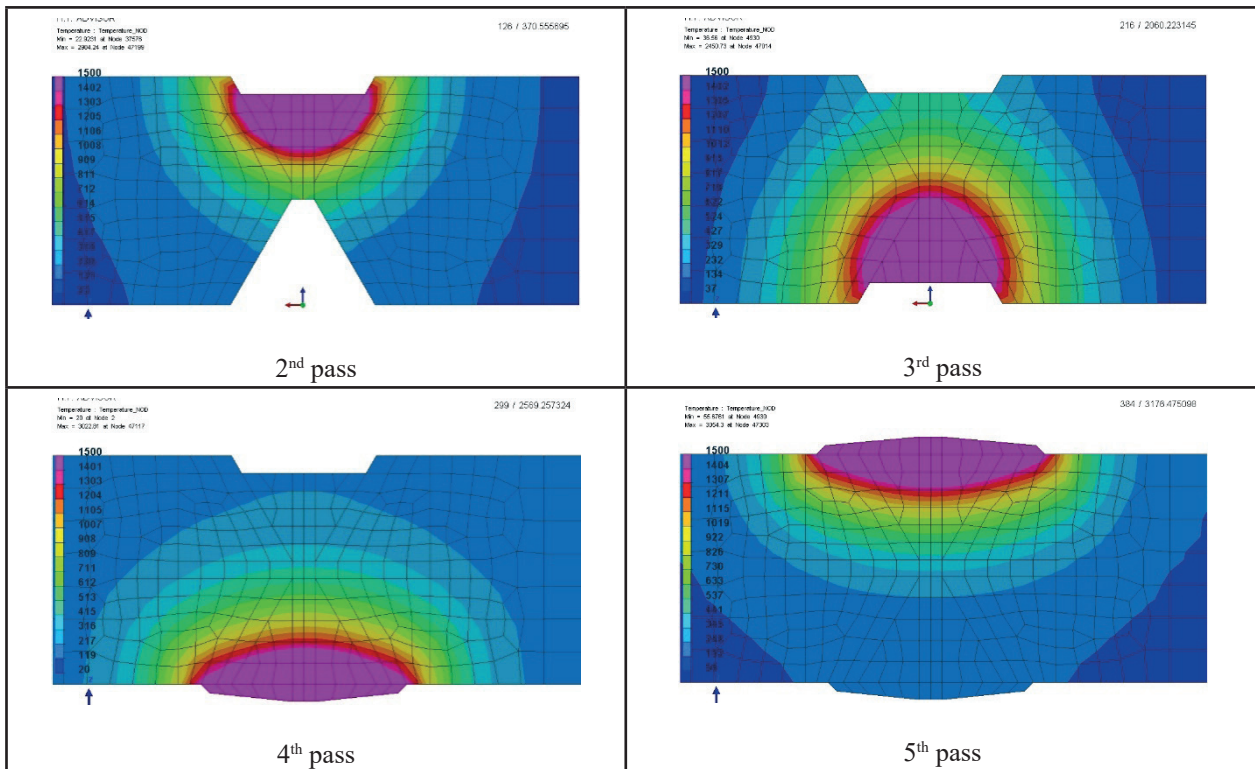


Fig. 5. Comparison of weld pool shapes for each weld pass during X2CrNiMoN22-5-3 butt joint welding

Simulation was a typical transient technique with thermo-metallurgical and mechanical analyses with parameters as in real welding technology including all parameters (for example interpass temperatures). Results of simulation were compared with real welding tests. Using the ‘Heat Input Fitting’ module helps to achieve proper shape of melted areas of each simulated beads what was confirmed with metallurgical investigation, Figs. 5 and 6.

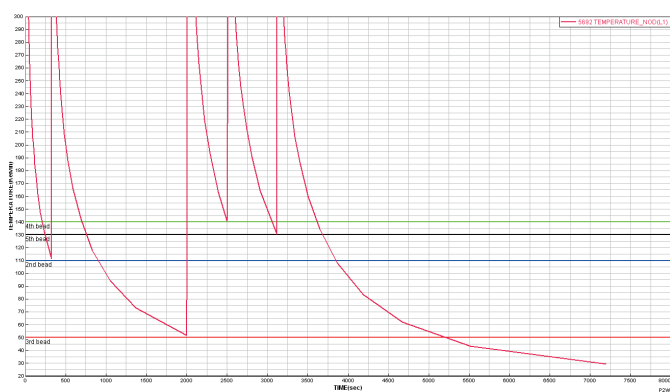


Fig. 6. Thermal cycle during welding with marked interpass temperatures of each bead

Results of mechanical analyses give a lot of information about stresses distribution and their values, Figs. 7-9. Analyses of reduced stresses (vonMises) indicate that maximal reduced stresses areas are directly at the bottom of welded bead. A maximal stress corresponds with mean stresses distribution calculated for each weld bead, Figs. 7-9.

Fig. 7. Stresses distribution on the surface and bottom of multipass welding of 20 mm thickness X2CrNiMoN22-5-3 steel butt weld joint

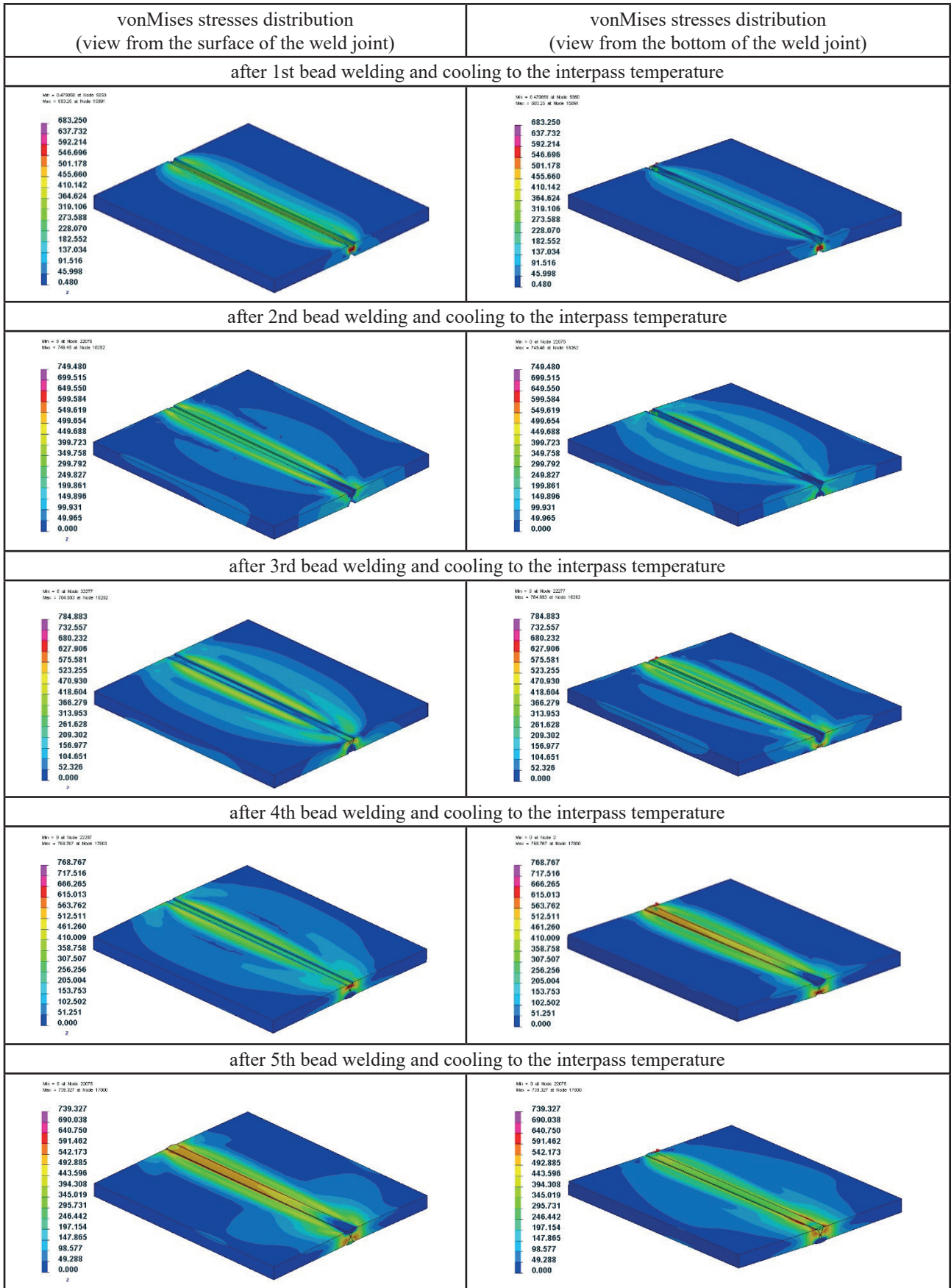
Mean stresses distribution corresponds with phenomena’s in multipass welding. There is a visible tensile and compressive stresses fields in the weld area and the influence of each next welded bead. Also max. level of distortions and the influence of welding from both sides is visible – for example between 4th and 5th pass – distortions were decreased due to the changes in stresses distribution, Fig. 8. Maximal level of residual stresses reached during the simulations is 784 MPa and it was observed in the weld and HAZ area after welding 3rd bead, Fig. 9. It is close but this value does not exceed literature and measured value of tensile strength, Table 3. This kind of results can be first warning for welding engineers during technology preparation that developed technology variant can be problematic in the real application.

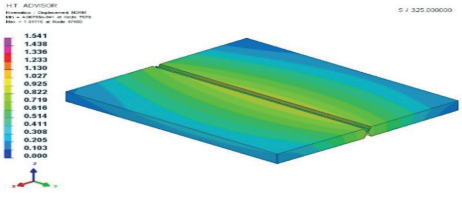
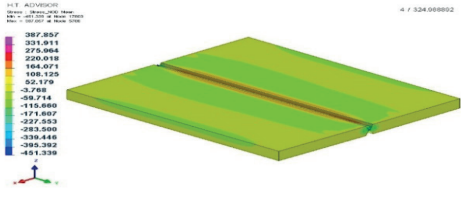
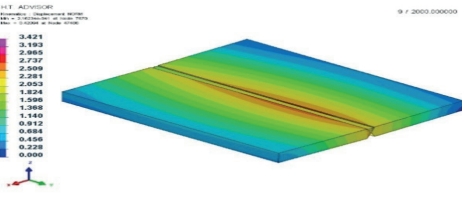
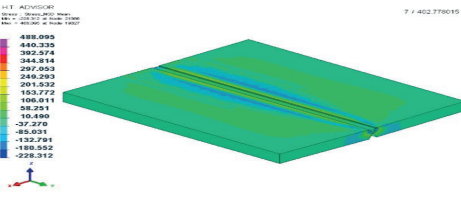
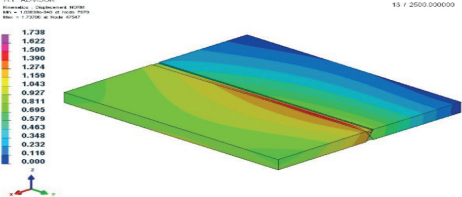
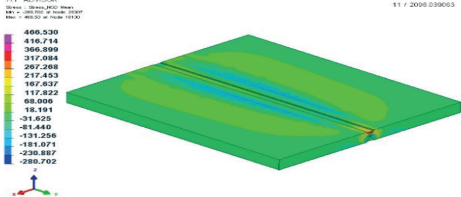
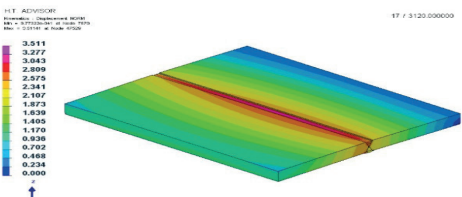
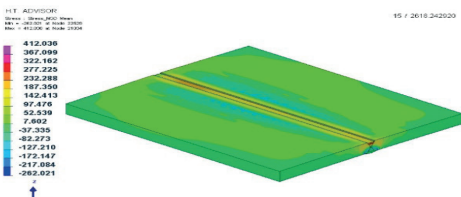
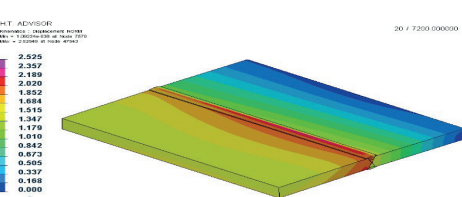
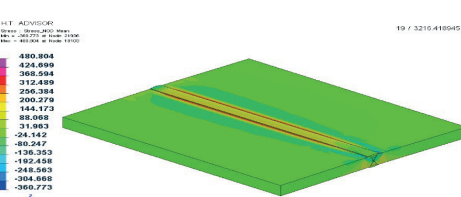
Fig. 8. Distortions and mean stresses distribution during and after multipass welding of 20 mm thickness X2CrNiMoN22-5-3 steel butt weld joint

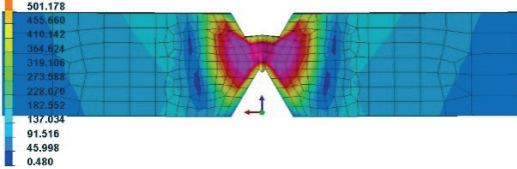
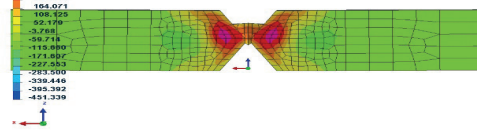
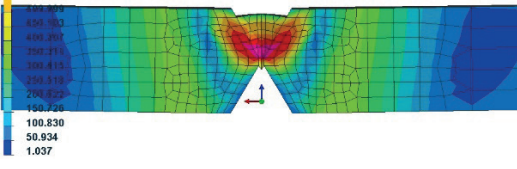
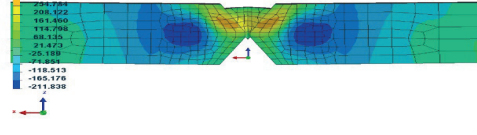
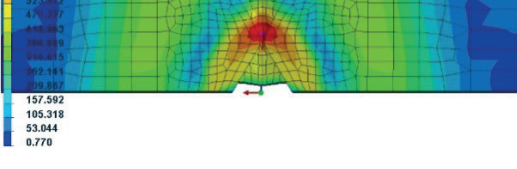
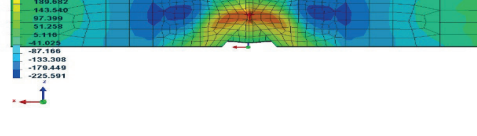
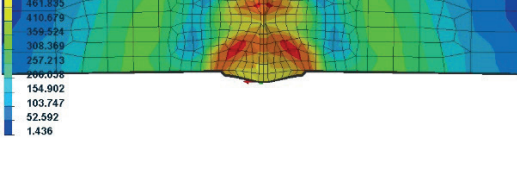
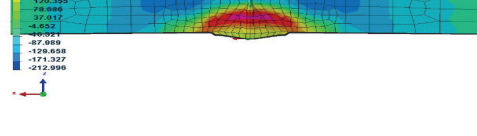
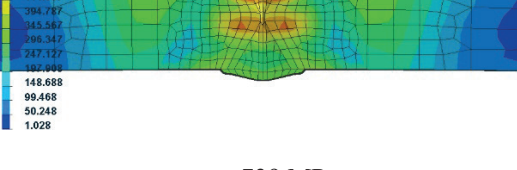
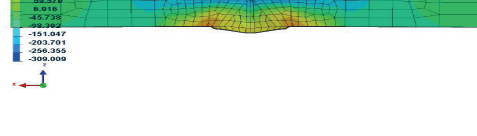
Fig. 9. VonMises and mean stresses on the cross section of weld during and after multipass welding of 20 mm thickness X2CrNiMoN22-5-3 steel butt weld joint

5. Conclusions

On the basis of the numerical analysis of X2CrNiMoN22-5-3 steel welding multipass butt joints it was possible to observe that results of numerical simulations corresponds well with for example mechanical properties tests. Of course it is needed to take into consideration that models



Distortions distribution (view from the surface of the weld joint)	Mean stresses distribution (view from the surface of the weld joint)
after 1st bead welding and cooling to the interpass temperature	
 <p style="text-align: center;">max. 1.54 [mm]</p>	 <p style="text-align: center;">min. -451 MPa, max. 387 MPa</p>
after 2nd bead welding and cooling to the interpass temperature	
 <p style="text-align: center;">max. 3.42 [mm]</p>	 <p style="text-align: center;">min. -228 MPa, max. 488 MPa</p>
after 3rd bead welding and cooling to the interpass temperature	
 <p style="text-align: center;">max. 1.74 [mm]</p>	 <p style="text-align: center;">min. -280 MPa, max. 466 MPa</p>
after 4th bead welding and cooling to the interpass temperature	
 <p style="text-align: center;">max. 3.51 [mm]</p>	 <p style="text-align: center;">min. -262 MPa, max. 412 MPa</p>
after 5th bead welding and cooling to the interpass temperature	
 <p style="text-align: center;">max. 2.52 [mm]</p>	 <p style="text-align: center;">min. -360 MPa, max. 480 MPa</p>

vonMises stresses distribution on the cross section	Mean stresses distribution on the cross section
after 1st bead welding and cooling to the interpass temperature	
 <p>Min = 0.47805 at Node 5000 Max = 683.25 at Node 15891</p> <p>683.250 637.732 592.214 546.696 501.178 455.660 410.142 364.624 319.106 273.588 228.070 182.552 137.034 91.516 45.998 0.480</p> <p style="text-align: center;">max. 683 MPa</p>	 <p>H.T. ADVISOR Date: 2009-03-04 10:00:00 User: 2009-03-04 10:00:00 Max. = 387.857 Min. = -451.339</p> <p>387.857 275.964 230.018 164.071 100.000 52.179 -3.765 -39.711 -115.080 -171.097 -227.114 -283.131 -339.148 -395.165 -451.182</p> <p style="text-align: center;">min. -451 MPa, max. 387 MPa</p>
after 2nd bead welding and cooling to the interpass temperature	
 <p>Min = 1.0221 at Node 720 Max = 749.48 at Node 16292</p> <p>749.480 699.584 649.688 599.792 549.896 499.999 450.103 400.207 350.311 300.415 250.519 200.623 150.726 100.830 50.934 1.037</p> <p style="text-align: center;">max. 749 MPa</p>	 <p>H.T. ADVISOR Date: 2009-03-04 10:00:00 User: 2009-03-04 10:00:00 Max. = 488.095 Min. = -211.538</p> <p>488.095 441.433 394.771 348.109 291.446 234.784 178.122 121.460 64.798 8.135 -52.523 -109.061 -165.599 -222.137</p> <p style="text-align: center;">min. -211 MPa, max. 488 MPa</p>
after 3rd bead welding and cooling to the interpass temperature	
 <p>Min = 0.76922 at Node 7556 Max = 784.88 at Node 11302</p> <p>784.883 732.008 680.134 628.260 576.386 524.512 472.637 420.763 368.888 317.014 265.139 213.265 161.390 109.516 57.641 0.770</p> <p style="text-align: center;">max. 784 MPa</p>	 <p>H.T. ADVISOR Date: 2009-03-04 10:00:00 User: 2009-03-04 10:00:00 Max. = 466.530 Min. = -225.591</p> <p>466.530 420.389 374.247 328.106 281.964 235.823 189.681 143.540 97.398 51.256 5.115 -40.925 -97.183 -153.341 -209.499 -265.657</p> <p style="text-align: center;">min. -225 MPa, max. 466 MPa</p>
after 4th bead welding and cooling to the interpass temperature	
 <p>Min = 1.40229 at Node 6970 Max = 768.76 at Node 11900</p> <p>768.767 717.611 666.456 615.301 564.145 512.989 461.833 410.679 359.524 308.369 257.213 206.058 154.902 103.747 52.592 1.436</p> <p style="text-align: center;">max. 768 MPa</p>	 <p>H.T. ADVISOR Date: 2009-03-04 10:00:00 User: 2009-03-04 10:00:00 Max. = 412.036 Min. = -212.098</p> <p>412.036 370.367 328.698 287.030 245.361 203.692 162.023 120.354 78.685 37.017 -4.652 -62.991 -121.638 -180.286 -238.934</p> <p style="text-align: center;">min. -212 MPa, max. 412 MPa</p>
after 5th bead welding and cooling to the interpass temperature	
 <p>Min = 1.02215 at Node 6870 Max = 739.32 at Node 11900</p> <p>739.327 690.107 640.887 591.667 542.447 493.227 444.007 394.787 345.567 296.347 247.127 197.907 148.688 99.468 50.248 1.028</p> <p style="text-align: center;">max. 739 MPa</p>	 <p>H.T. ADVISOR Date: 2009-03-04 10:00:00 User: 2009-03-04 10:00:00 Max. = 480.808 Min. = -309.059</p> <p>480.808 428.150 375.492 322.834 270.176 217.518 164.860 112.202 59.544 6.886 -45.732 -102.080 -159.422 -216.764 -274.106 -331.448</p> <p style="text-align: center;">min. -309 MPa, max. 480 MPa</p>

are always more ideal than real life but still we obtain high accuracy of results level.

As was said, maximal level of residual stresses reached during the simulations was 784 MPa (in the weld and HAZ area after welding 3rd bead). It is close but this value does not exceed literature and measured value of tensile strength but it is an information to the engineers that developed technology variant can be problematic in the real application.

Of course these results can be little different according to real situation because of using material database with ferrite/austenite content as 50/50. In real tests of dual-phase steel welding significant percentage amount of this two phases were observed. Except the quantitative changes, also phases morphology and existing areas can change. On the boundary of base material and HAZ can exist big areas of ferrite, again on the boundary between HAZ and weld – austenite enriched areas were dominated.

Summary, numerical analysis enables faster and cheaper selection of the optimum manner of fixing elements, interpass temperatures etc. for welding as well as the precise analysis of stress and strain distributions also during the welding. As a result, numerical analysis makes it possible to significantly reduce prototyping costs and to consider a greater number of possible solutions without risking additional costs. This method also enables the analysis of difficult and expensive issues as regards necessary testing equipment.

Works were done during realization:

Project POIG.01.04.00-04-206/12 funded as a part of Operational Program Innowacyjna Gospodarka, lata 2007 ÷ 2013, Priorytet 1. Badania i rozwój nowoczesnych technologii, Działanie 1.4. Wsparcie projektów celowych”

REFERENCES

- [1] T. Kik, Numerical analysis of MIG welding of butt joints in aluminium alloy, *Biuletyn Instytutu Spawalnictwa* **58**, (3), 37-49 (2014).
- [2] M. Slováček, T. Kik, Use of Welding Process Numerical Analyses as Technical Support in Industry. Part 1: Introduction to Welding Process Numerical Simulations, *Biuletyn Instytutu Spawalnictwa* **59**, (4), 25-31 (2015).
- [3] T. Padma Kumari, S. Venkata Sairam, Finite Element Analysis of EBW Welded Joint Using SYSWELD. *International Journal of Emerging Technology and Advanced Engineering* **3**, (2), 335-340 (2013).
- [4] T. Kik, M. Slováček, J. Moravec, M. Vaněk, Numerical Analysis of Residual Stresses and Distortions in Aluminium Alloy Welded Joints, *Applied Mechanics and Materials* **809-810**, 443-448 (2015).
- [5] F. Kong, J. Ma, R. Kovacevic, Numerical and experimental study of thermally induced residual stress in the hybrid laser–GMA welding process, *Journal of Materials Processing Technology* **211**, 1102–1111 (2011).
- [6] Ch. Liu, J. Zhang, B. Wua, S. Gong, Numerical investigation on the variation of welding stresses after material removal from a thick titanium alloy plate joined by electron beam welding, *Materials and Design* **34**, 609–617 (2012).
- [7] J.A. Goldak, A. Oddy, M. Gu, W. Ma, A. Mashaie, E. Hughes, Coupling heat transfer, microstructure evolution and thermal stress analysis in weld mechanics, *IUTAM Symposium. Mechanical Effects of Welding*, June 10-14, Lulea Sweden, (1991).
- [8] C.S. Wu, H. G. Wang, Y. M. Zhang, A new heat source model for keyhole plasma arc welding in FEM analysis of the temperature profile, *Welding Journal* **85**, (12), 284–291 (2006).
- [9] J. Goldak, V. Breiguine, N. Dai, J. Zhou, Thermal stress analysis in welds for hot cracking. ASME, Pressure Vessels and Piping Division PVP. *Proceeding of the 1996 ASME PVP Conf.*, July, 1-26, Montreal (1996).
- [10] *Welding simulation user guide, Sysweld manual*, ESI Group, (2016).
- [11] T. Giętka, K. Ciechacki, M. Chudziński, Kryteria wyboru technologii spawania zbiornika magazynowego, *Inżynieria i Aparatura Chemiczna* **51**, (5), 219-220 (2012).
- [12] K. Ciechacki, T. Giętka, M. Chudziński, Zastosowanie stali duplex w przemyśle spożywczym, *Inżynieria i Aparatura Chemiczna* **52**, (2), 122-124 (2013).

